Highlights

- *P-E* relationships were measured monthly in 2003 for total and large phytoplankton
- Different photosynthetic performance showed little photoacclimation in large cells
- Water-column production to biomass was only predictable for large phytoplankton
- Low annual primary production (139 g C m^{-2} y^{-1}) was due to nutrient limitation

A paper submitted to *Estuarine, Coastal and Shelf Science*
v2 (Nov 19th 2014)

Photosynthetic parameters and primary production, with focus on large phytoplankton, in a temperate mid-shelf ecosystem

Xosé Anxelu G. Morán[1,2] * and Renate Scharek[1]

[1] Red Sea Research Center, King Abdullah University of Science and Technology, 23955-6900 Thuwal, Saudi Arabia

[2] Centro Oceanográfico de Xixón, Instituto Español de Oceanografía Camín de L'Arbeyal s/n, E-33212 Xixón, Asturies, Spain

*Corresponding author: xelu.moran@kaust.edu.sa

Abstract

Annual variability of photosynthetic parameters and primary production (PP), with special focus on large (i.e. >2 µm) phytoplankton was assessed by monthly photosynthesis-irradiance experiments at two depths of the southern Bay of Biscay continental shelf in 2003. Integrated chl *a* (22-198 mg m^{-2}) was moderately dominated by large cells on an annual basis. The March through May dominance of diatoms was replaced by similar shares of dinoflagellates and other flagellates during the rest of the year. Variability of photosynthetic parameters was similar for total and large phytoplankton, but stratification affected the initial slope α^B [0.004-0.049 mg C mg chl a^{-1} h^{-1} (µmol photons m^{-2} $s^{-1})^{-1}$] and maximum photosynthetic rates P^B_m (0.1-10.7 mg C mg chl a^{-1} h^{-1}) differently. $P^B_{m,}$ correlated positively with α^B only for the large fraction. P^B_m tended to respond faster to ambient irradiance than α^B, which was negatively correlated with diatom abundance in the >2 µm fraction. Integrated PP rates were relatively low, averaging 387 (132-892) for the total and 207 (86-629) mg C m^{-2} d^{-1} for the large fraction, likely caused by inorganic nutrient limitation. Although similar mean annual contributions of large phytoplankton to total values were found for biomass and PP (~58%), water-column production to biomass ratios (2-26 mg C mg chl^{-1} d^{-1}) and light utilization efficiency of the >2 µm fraction (0.09-0.84 g C g chl^{-1} mol $photons^{-1}$ m^2) were minimum during the spring bloom. Our results indicate that PP peaks in the area are not necessarily associated to maximum standing stocks.

Keywords: phytoplankton; photosynthesis-irradiance relationships; primary production: size; annual variations; Bay of Biscay

Running head: Large cells photosynthesis and primary production

INTRODUCTION

Phytoplankton is the foundation of marine food webs in pelagic waters and consequently its biomass, usually expressed as chlorophyll *a* concentration, is widely used as an indicator of ecosystem productivity and trophic status. However, photosynthetic carbon fixation is also dependent on light, nutrient availability and community composition among other factors, indirectly related to standing stocks. In temperate waters the predictable nature of the first two factors associated with seasonal variations in water column stability also influence largely the composition of phytoplankton dominant assemblages (e.g. Cullen et al., 2002). However, due to the transient nature of phytoplankton blooms, changes in community composition are much more difficult to predict than most physico-chemical properties. A marked dominance of chain forming diatoms in the algal blooms occurring in late winter-early spring and autumn in temperate coastal waters is well documented (Ianson et al., 2001; Winder and Cloern, 2010). For the rest of the year, non-diatomeous pico- and nanophytoplankton and occasionally big dinoflagellates (Cullen et al., 2002) dominate. Reports on seasonal changes in bulk and size-fractionated biomass and community composition have increased largely over the last decades. Fewer descriptions of complete annual cycles of pelagic photosynthesis and primary production are available. In European waters, the studies we are aware of are mostly restricted to inshore waters (Cermeño et al., 2006; Gameiro et al., 2011; Marty and Chiavérini, 2002; Tillmann et al., 2000).

Photosynthesis-irradiance relationships or *P-E* curves are a convenient and widespread way of describing the physiological and acclimation response of phytoplankton assemblages to environmental changes (Sakshaug et al., 1997). Previous research has shown that photosynthetic parameters differ in the time-scales of response to new conditions established within the water column (Lewis et al., 1984). For instance, Geider (1993) noticed that stratification triggers changes in maximum chlorophyll normalized photosynthetic rate (P^B_m) but is usually less visible in the slope of the light-limited region (α^B), claimed to be more constant than the former parameter (Behrenfeld *et al.*, 2004, but see Cullen and Lewis, 1988). The frequent covariation of both photosynthetic parameters, extensively reviewed by (Behrenfeld *et al.*, 2004), has intrigued aquatic phycologists, but we still lack a complete mechanistic explanation for the so-called E_k-independent (i.e. strong positive correlation between P^B_m and α^B) or E_k-dependent (no P^B_m-α^B covariation) variability. Saturation irradiance (E_k) in turn frequently reflects current or recent light regimes (Tilstone et al., 2003).

Butrón *et al.* (2009) have reviewed available studies on size-fractionated phytoplankton biomass and primary production in nearshore and estuarine ecosystems of the Bay of Biscay, but we lack information about offshore waters. They concluded that bays and the outer areas of large estuaries usually exhibit marked phytoplankton peaks in spring, when the most favourable conditions for the development of phytoplankton are attained, since irradiances are high enough by that time and nutrients can become limiting in summer. However, on an annual basis riverine nutrient inputs are sufficient to sustain dominance by large (i.e. >2 µm) cells. In the southern Bay of Biscay´s open continental shelf, an annual cycle of photosynthetic carbon fixation by picophytoplankton and its relationship with community structure and growth rates were already described in Morán (2007), who concluded that roughly half of total primary production was accounted for by the smallest size-class. Here, we focus on the photosynthetic performance of large cells and the whole phytoplankton assemblage. The objectives of this study are i) to describe and analyze seasonal variations in photosynthetic performance and primary production rates of total phytoplankton and the fraction >2 µm in relation to water-column properties, and ii) to explore the potential of intra-annual variability for predicting the total amount of organic carbon entering the food web using chlorophyll and environmental variables.

METHODS

Environmental variables

Physico-chemical variables were measured and biological samples were collected at a continental shelf station (43.7ºN, 5.6ºW, 110 m depth) from January to December 2003 as detailed in (Morán, 2007). This is the central station of the monthly RADIALES transect off Xixón in the central Cantabrian Sea (southern Bay of Biscay) on board the RV 'José de Rioja. Vertical profiles of temperature and salinity were obtained with a SeaBird 25 CTD probe and photosynthetically active radiation (PAR, 400-700 nm) was measured with a Biospherical QSP-2200 spherical quantum sensor. After calculation of the vertical light extinction coefficients (K_d), optical depths (ζ) for the water samples taken for the photosynthetic parameters experiments were determined as K_d z, with z as the original depth. Actual daily surface irradiance (PAR) on the date of the monthly experiments (E_0) was measured with a LI-192SA (LI-COR) quantum sensor, ranging from 10.0 and 38.4 mol photons m^{-2} d^{-1}. Additionally, climatological monthly values of PAR based on horizontal insolation averaged for 22 years (NASA) were used as the expected irradiance at the surface without cloud cover ($E_{0\ exp}$). These values were

higher than the measured E_0 with heavily overcast skies on three occasions, but otherwise there was a very good correspondence between both surface daily PAR estimates (r=0.99, p<<0.001, n=9).

For chlorophyll *a* concentration (chl *a*), 100 ml samples taken at 8 discrete depths (0, 10, 20, 30, 40, 50, 75 and 100 m) were sequentially filtered through 20, 2 and 0.2 µm Millipore polycarbonate filters (47 mm diameter). The filters were kept frozen at -20°C until analysis. Usually within 1 wk they were then placed in 90% acetone at 4°C for 24 h and the fluorescence of the extract was measured without acidification using a Perkin Elmer LB-50s spectrofluorometer (excitation at 440 nm, emission at 685 nm), periodically calibrated with pure chl *a* solution. Chl *a* in the picoplanktonic, nanoplanktonic, and microplanktonic size fractions was estimated as the the amounts retained on the 0.2, 2 and 20 µm filters, respectively. Additionally, 100 ml chl *a* samples from the two depths of the *P-E* relationships determinations were taken and processed as detailed in Morán (2007). Samples for analyzing nitrite, nitrate, phosphate and silicate were immediately frozen and their concentrations determined in the laboratory with a Technicon autoanalyzer following standard procedures (Grasshoff *et al.*, 1999).

Large phytoplankton community composition

Samples for large (large nano- plus microplankton) phytoplankton community composition were taken monthly at 0, 30 and 75 m. 100 ml were collected in brown glass bottles, preserved with acid Lugol's solution and kept in the dark until analysis under an inverted microscope using the (Utermöhl, 1958) technique. Diatoms, dinoflagellates, flagellates and ciliates were quantified and differentiated into size classes. Interpolation was used for deriving the abundance of the 4 broad taxonomical groups at the depth of the subsurface chlorophyll maximum when sampling depths were not coincident with those of the *P-E* experiments. Integrated abundances from 0 to 75 m were also calculated (cells m^{-2}). Total phytoplankton includes the picoplanktonic groups analyzed by flow cytometry and described in detail in Morán (2007). Some small cells within the nanoplankton size-class (i.e. 4-8 µm in diameter) may have been missed by combining both counting methods but we believe that total cell number estimates were close to actual values.

Photosynthetic parameters

Samples for the *P-E* experiments were collected at ca. 2 m and the depth of the subsurface chl *a* maximum (Morán 2007), hereinafter referred to as "surface" and "deep". Full details of the experimental setup, irradiance measurements within the

incubator and sample processing are given in Morán (2007). The method used for separating large (nano- plus microphytoplankton) from picophytoplankton carbon fixation involved specific *P-E* curve fitting for three fractions, total, >2 and <2 µm. Two different models were used to fit chl *a*-normalized hourly primary production rates, depending on the presence (Platt *et al.*, 1980), Eq. 1) or absence of photoinhibition (Webb *et al.*, 1974), Eq. 2):

$$P^B = P^B_s [1 - \exp(-\alpha^B E/P^B_s)] [\exp(-\beta^B E/P^B_s)] \quad \text{Eq. (1)}$$

$$P^B = P^B_m [1 - \exp(-\alpha^B E/P^B_m)] \quad \text{Eq. (2)}$$

in which P^B is the chl.*a*-normalized photosynthetic rate (mg C mg chl a^{-1} h^{-1}), P^B_m is the maximum chl.*a*-normalized photosynthetic rate (same units as P^B*;* P^B_m is calculated as $[P^B_m \times (\alpha^B / (\alpha^B + \beta^B) \times (\beta^B / (\alpha^B + \beta^B)]^{\beta B/\alpha B}$ in Platt's et al. model, with P^B_s as the maximum chl.*a*-normalized photosynthetic rate without photoinhibition), α^B is the initial, light-limited slope [mg C mg chl a^{-1} h^{-1} (µmol photons m^{-2} $s^{-1})^{-1}$], β^B is the photoinhibition parameter (same units as α^B), E is the experimental irradiance (µmol photons m^{-2} s^{-1}) and E_k is the saturation irradiance, (same units as E and calculated as P^B_m / α^B).

Primary production

Vertical distributions of chl *a* (total and large fractions) and PAR were used with the corresponding photosynthetic parameters for estimating volumetric primary production rates at the different depths of the water column. Linear interpolation of photosynthetic parameters was used between surface and deep values and extrapolation of the latter values down to 75 m. Finally, trapezoidal integrations were made for the upper 75 m of the water column rather than the euphotic zone in order to allow better assessments of the role of large phytoplankton group composition in measured rates. The euphotic zone depths during 2003 was always shallower than the depth of integration, ranging from 27 (April) to 74 m (August).

Statistics

P-E model fitting was performed with the non-linear option of KaleidaGraph software (v. 3.0). All other statistics (correlation analyses, ordinary least-squares linear regressions, paired *t*-tests and polynomical fitting for better showing seasonal patterns) were performed with Statistica software (v. 7.1).

RESULTS

Environmental conditions

Detailed descriptions of environmental properties at the study site during 2003 are given elsewhere ((Morán, 2007). Briefly, temperature and salinity seasonal variations induced changes in the upper mixed layer depth, which extended down to the bottom (110 m) in December and was usually shallowest (<15 m) in summer while the euphotic layer remained more stable year-round (51 ± 17 m, mean and SD). From June through October, the water column was stratified as indicated by stratification index values >0.01 kg m^{-4} (roughly equivalent to >0.05ºC m^{-1}). Vertical distributions of nutrient concentrations tended to reveal a similar seasonal pattern, except that the development of the phytoplankton bloom in spring decreased phosphate and nitrate concentrations in the upper layers to annual minima from March through summer. (Table 1, see also Fig. 1D in Morán, 2007 for nitrate). Silicate concentrations (Table 2) in the upper layers showed similar seasonal patterns as phosphate and nitrate and concentrations and surface winter molar ratios of nitrate-nitrite to silicate concentrations were between 1 and 2. Total chlorophyll *a* concentrations in the euphotic layer ranged from 0.06 to 3.89 mg m^{-3}, with subsurface maxima usually located between 20 and 40 m depth, except in June and July, when they were found slightly deeper at 50 m (see Fig. 1C in Morán, 2007). As indicated by chl *a* size fractionation, large phytoplankton (>2 µm) dominated the community year-round with only 3 months of picophytoplankton dominance (August, October and November, Morán, 2007). Within the large fraction, the relative contribution of nanoplankton was generally much higher than that of microplankton (mean annual values of 40 % ± 11% SD and 18% ± 18%, respectively), with dominance of microplankton only in March and April (~57%). During the rest of the year, microplankton contributions were generally <10%.

The broad groups of large phytoplankton varied seasonally (Fig. 1), with a marked dominance of diatoms during the winter-spring transition, exceeding 1.8 x 10^9 cells m^{-2}. In April diatoms made up as much as 93% of total cell numbers of large phytoplankton integrated down to 75 m, while dropping to 2% in August and December. Contribution of other groups was less variable, with dinoflagellates slightly more abundant than other flagellates, mostly big nanoflagellates (10-20 µm) on an annual basis (36 vs. 28%). Both groups clearly dominated the community for the second half of the year, with ciliates (including potentially mixotrophic species) contribution close to 20% from July through November. The diatom to dinoflagellate cell abundance ratio varied accordingly from 0.03 in December to 22 in April. Values greater than 1 were observed from March through May and also in July.

Photosynthetic parameters

The initial slope of the *P-E* curve (α^B) ranged from 0.004 to 0.049 mg C mg chl a^{-1} h^{-1} (µmol photons m^{-2} $s^{-1})^{-1}$, with almost the same ranges of variation for the total and large fraction (Fig. 2A, B). However, while surface and deep values of large phytoplankton were not significantly different year-round, α^B of total phytoplankton was greater at depth from July through November, coincident with the period of summer stratification (Fig. 2B, paired *t*-test p=0.007, n=5).

Maximum photosynthetic rates were also similarly variable for both size fractions (0.20 – 9.78 for the large and 0.13 – 10.68 mg C mg chl a^{-1} h^{-1} for the total), characterized by relative maxima in summer at the surface and minima in June deep samples (Fig. 2C, D). Surface P^B_m values were consistently greater than at depth (paired *t*-tests, p=0.02 for total and <0.001 for >2 µm phytoplankton, n=12).

Photoinhibition was detected only in summer (0.22-18.2 10^{-4} mg C mg chl a^{-1} h^{-1}) with increasing values from June through August for both total and large phytoplankton, and 3-fold higher values on average for large cells.

Saturation irradiance of surface samples was seasonally more variable for total phytoplankton than for the large fraction, with higher values during summer higher irradiances (Fig. 2 F). Except in July (Fig. 2F), actual mean surface irradiances were generally much higher than E_k values, indicating year-round light-saturated photosynthesis in the upper layers. In contrast, mean irradiances at depth were always lower than the corresponding E_k values (Fig. 2E, F), although they were positively correlated for both large and total phytoplankton (r=0.74 and 0.80, p=0.002 and 0.006, respectively, n=12).

Largely due to the different behaviour of α^B and P^B_m during summer stratification in bulk assemblages (Fig 2B, D), no covariance was observed for total phytoplankton, neither for the entire dataset nor any depth subset. However, for large phytoplankton these photosynthetic parameters were positively correlated both in surface (r=0.77, p=0.003, n=12) and deep (r=0.66, p=0.02, n=12) samples, and with all data pooled (Fig. 3A). Large phytoplankton α^B values were also significantly and negatively correlated with the absolute abundance of diatoms, with surface and deep data showing the same pattern (Fig. 3B).

With all data pooled, P^B_m and E_k were negatively correlated with optical depth for both total and large phytoplankton (Fig. 4B, C). While α^B bore no significant correlations, the signs were opposite in the two groups, negative for cells >2 µm and positive for the total assemblage, due to the significant positive correlation when only picophytoplankton data were considered (Fig. 4A, see also Morán, 2007). Although the time-scale available for light acclimation differs for mixed and stratified waters, the relationships shown in Fig. 4 were essentially the same when the dataset was split in the two periods (data not shown).

Primary production

As expected, volumetric primary production rates consistently decreased vertically (data not shown). Integrated (0-75 m) values (Table 2) ranged from 127 to 896 and 88 to 545 mg C m^{-2} d^{-1} for total and the large fraction, respectively. Both total areal biomass and productivity were significantly correlated with the contribution of large cells to the phytoplankton assemblage, measured as the number of cells >2 µm, and the importance of diatoms, either as absolute abundance or the diatom-to-dinoflagellate ratio (r=0.73-0.98, p<0.008, n=12).

Mean annual values of the integrated contribution of large phytoplankton to total biomass (BL/BT) and production (PL/PT) were virtually the same (paired *t*-test, p=0.93, n=12) but they showed a slightly different seasonality, with BL/BT ratios consistently higher than PL/PT from February to May (Table 2). While BL/BT was significantly correlated with K_d (r=0.71, p=0.01, n=12), PL/PT increased with higher phosphate concentrations, both at the surface (r=0.85, p=0.001, n=11) and averaged for the upper 75 m (Table 2, r=0.76, p=0.007, n=11).

Corresponding integrated primary production to chlorophyll ratios (PP/Chl) varied over one order of magnitude (2.3-23.3 mg C mg chl^{-1} d^{-1}) and were similar for total and >2 µm phytoplankton (Table 2, paired *t*-test, p=0.69). $PP/Chl_{>2\ \mu m}$ increased with stratification index (r=0.65, p=0.02, n=12,) while PP/Chl_{tot} was significantly correlated with measured daily irradiance at the surface E_0 (r=0.59, p=0.03, n=12). Variability in PP/Chl ratios was thus seasonally predictable, especially for the large fraction, and when PP calculations considered the expected, climatological surface irradiance ($E_{0\ exp}$) rather than actual measurements (E_0). This new variable ($E_{0\ exp}$ PP/Chl ratio) corrected for the very low irradiances measured in June and especially in July 2003, due to overcast conditions (see Fig. 2E and F). Although for the rest of the year E_0 values were virtually the same as $E_{0\ exp}$, 12 mol photons m^{-2} d^{-1} measured in July were far

below the expected value of 48 mol photons m^{-2} d^{-1} (similarly, 34 vs. 47 mol photons m^{-2} d^{-1} in June). $E_{0\ exp}$ PP/Chl maxima were generally attained in summer while minima characterized winter and autumn (Fig. 5A). A strong positive relationship was found between its values and stratification index (Fig. 5B).

Since PP/Chl ratios covaried positively with surface irradiance, when corrected by E_0, yielding Ψ, the water-column light utilization efficiency as defined by (Falkowski, 1981), variability of Ψ values of total and large phytoplankton was similar (0.13-0.88 and 0.09-0.81 mg C mg chl^{-1} mol $photons^{-1}$ m^{-2}, respectively, Fig. 6) but only the latter showed a consistent seasonal pattern. $\Psi_{>2\ \mu m}$ was significantly correlated with mean phosphate concentrations in the 0-75 m depth interval used for calculations (Table 2, r=0.67, p=0.03, n=11).

Discussion

Photosynthetic performance of total and large phytoplankton

Our results indicate that the photosynthetic behaviour of bulk phytoplankton assemblages (Fig. 2B, D, F) is a combination of the different strategies of the two size fractions examined, large (>2 µm, this work) and small (<2 µm, (Morán, 2007). For instance, the overall higher values of α^B at depth during summer stratification were largely attributable to picophytoplankton (Morán 2007) since large phytoplankton values were essentially undistinguishable at the two depths (Fig. 2A). Table 1 shows significantly higher values of picophytoplanktonic α^B and P^B_m compared with the larger fraction at depth. Higher values of both photosynthetic parameters in small phytoplankton compared with the large fraction were similar to other temperate coastal water surveys (Frenette et al., 1996; Joint and Pomroy, 1986; Platt et al., 1983), a feature different from open-ocean, strongly oligotrophic waters (Fernández et al., 2003).

On an annual basis large phytoplankton maximum photosynthetic capacity covaried with the initial slope (Fig. 3A), thus showing "E_k-independent variability" (Behrenfeld et al., 2004), although some acclimation of E_k was still observed especially on the vertical scale (Fig. 4C) rather than temporally (Fig. 2E). Our data thus suggest that E_k-independent variability can only be expected for large cells or in regions and periods in which phytoplankton is clearly dominated by the largest size-classes (Basterretxea and Arístegui, 1999; Claustre et al., 1997; Morán and Estrada, 2001). In their study of potential physiological mechanisms for this phenomenon, (Behrenfeld *et al.*, 2004) did

not assess the specific role of cell size. Differential metabolic pathways in photosynthetic prokaryotes (<2 µm) and eukaryotes (found in all size classes) responsible for the balance between reductants and ATP generation (Behrenfeld et al., 2004) cannot be excluded. Although the reason for this observation remains elusive, larger cells are more prone to modify α^B and P^B_m in the same direction in response to a changing light environment than small cells, which changed P^B_m and α^B in opposite directions when the water-column of the study site was strongly stratified (Morán, 2007).

The vertical photoacclimation of the maximum photosynthetic rate was much more robust and widespread than the other photosynthetic parameters (Fig. 4). Similar to winter-spring observations in the NW Mediterranean (Morán and Estrada, 2005), we failed to find any significant pattern of the initial *P-E* slope on an annual basis for either large or total phytoplankton (Fig. 4A), contrary to previous work reporting increasing α^B values deeper in the water column (Basterretxea and Arístegui, 2000; Dower and Lucas, 1993; Morán et al., 2001) or, less frequently, decreasing (Morán and Estrada, 2001). Surface assemblages generally lie closer to P^B_m rather than spend too much time on the light-limited region and E_k was almost always well below daily irradiance (Fig. 2E, F) as found elsewhere (e.g. (Côté and Platt, 1983). On the contrary, E_k values at depth were considerably higher than measured irradiances indicating light-limited conditions although probably mixing made cells spend some time at shallower depths. However, deep E_k values significantly followed changes in the light field (Fig. 2E,F), suggesting that there both large and small phytoplankton communities were able to adjust E_k in a similar fashion, in contrast to the α^B parameter (cf. Fig. 4A and C). In any case, the slope of the linear regression between P^B_m and α^B (125 µmol photons m^{-2} s^{-1}, Fig. 3A) summarizes the year-round E_k–independent variability of large phytoplankton. Although differences between surface and deep E_k values were also detected during stratification in the >2 µm fraction (Fig. 2E), they were much larger when the total assemblage was considered (Fig. 2F). All in all, large phytoplankton showed little photoacclimation (MacIntyre et al., 2002) compared with picophytoplankton (Morán 2007) even in stratified conditions, as also noted by (Uitz *et al.*, 2008).

Primary production rates

Since the introduction of the ^{14}C technique by (Steemann-Nielsen, 1952), thousands of measurements of pelagic primary production have been performed. However, the seasonal patterns, accounting for a large fraction of its variability in mid- to high latitude ecosystems, are only well known for a few sites of the world ocean. Our total primary

production rates were generally low to moderate in 2003 with the exception of April (Table 2). Although we observed a marked diatom bloom in that month (Fig. 1), total PP did not even reach 1 g C m^{-2} d^{-1}, far from the values measured during the winter-spring blooms in more productive areas nearby such as the Galician Rías (e.g.(Cermeño et al., 2006; Ospina-Alvarez et al., 2014; Varela et al., 2005) or even in the NW Mediterranean (Estrada, 1996; Morán and Estrada, 2005) and refs. therein), traditionally regarded as a more oligotrophic ecosystem. However, our total annual primary production estimate of 139 g C m^{-2} y^{-1} is well in agreement with 37 year hindcasted values along the Bay of Biscay continental shelf (Huret et al., 2013). With the limitation of just one year of sampling, this primary production rate would place the mesotrophic southern Bay of Biscay (Cantabrian Sea) continental shelf closer to oligotrophic conditions (Cullen et al., 2002; Nixon, 1995), especially if we take also into account the measurements made at a mid-shelf station off Cuideiru, located ca. 50 km eastwards of Xixón, which for the 1992-2007 period were considerably lower than our values (mean 83 mg C m^{-2} d^{-1}, (Bode *et al.*, 2011). We cannot discard substantially higher annual primary production rates at the study site in other years because of the anomalously low SiO_2 concentrations measured in 2003 (e.g. in 2004 mean concentrations in the 0-75 m layer were more than double). Although both α^B and P^B_m values were twice as high for picophytoplankton than for the large fraction at depth (Table 1), especially during stratification (cf. Fig. 2 and Fig. 4 in Morán 2007), with a mean annual value of 75 g C m^{-2} y^{-1}, production by large phytoplankton slightly dominated over that of small cells in the upper 75 m (Table 2).

Phytoplankton standing stocks are frequently used as proxies of productivity (e.g.(Boyce et al., 2010; Falkowski et al., 1998; Vollenweider et al., 1998), and indeed off Xixón both variables covaried positively both for the total and the large fraction, although the correlation was only significant for total phytoplankton (r=0.70, p=0.011, n=12). However, environmental controls differed when a complete seasonal cycle was considered. For instance, although sharing a mean annual value of ~58% (Table 2), it was the variable large cells relative production rather than biomass that correlated positively with inorganic nutrient concentrations (significantly only for phosphate). Furthermore, dissimilar patterns of BL/BT and PL/PT were identified for spring in comparison to the rest of the year, which was probably related to the different specific composition of large phytoplankton assemblages. From March through May, BL/BT values >0.60 (Table 2) due to annual maximum abundances of diatoms (Fig 1), were characterized by a constant, rather low PL/PT value of 0.46. These values might have been greater had we sampled algal blooms at the initial rather than the decay phases

probably characterizing our samples. However, this pattern may also be a consequence of the decrease in the light utilization efficiency parameter (α^B) with increasing diatom contribution found for all monthly data (Fig. 3B). On the other hand, PL/PT peaks in June, September and December corresponded to very different assemblage conditions. While the September peak in absolute and relative diatom abundance (Fig. 1) could suggest that the sporadic autumn blooms were more efficient than spring blooms (Figs. 5A and 6), June and December samples shared a virtually equal contribution of flagellates and dinoflagellates (Fig. 1), with the highest abundances of the latter group recorded in 2003 ($1.2\ 10^9$ cells m^{-2}). The lowest annual contribution of diatoms found in December suggests that this group does not need to be present for large cells dominance of primary production (Tremblay and Legendre, 1994).

Water-column assimilation numbers or PP/chl ratios varied from 2 to 26 and from 5 to 22 g C g chl^{-1} d^{-1} for large and total phytoplankton, respectively (Table 2), well within reported ranges (Falkowski, 1981) and seasonality similar to other temperate regions, with minima in autumn and winter and maxima in early summer (Jouenne et al., 2007; Shaw and Purdie, 2001; Tillmann et al., 2000). When the expected rather than measured irradiance (i.e. without cloud cover) was used, predictability of PP/chl>2 was very strong (Fig 5A), which would allow us to estimate monthly areal production rates of large phytoplankton from just biomass measurements if future investigations confirm the marked seasonal pattern found. Vertical changes in production rates were much more marked than in biomass, resulting in negative exponential decreases of PP/Chl ratios vs. depth (from -0.05 to -0.16 m^{-1}) that became steeper with higher K_d values ($r=0.98$, $p<<0.01$, $n=12$), thus illustrating the major role played by underwater irradiance. This can help explain the perhaps counterintuitive fact that summer maximum $PP/chl_{>2\ \mu m}$ ratios were 10-fold larger than April values (Table 2) where the highest monthly PP was measured. A shading effect due to accumulated biomass and a ca. 4-fold decrease in α^B (Fig. 3B) may be behind the decrease in $PP/Chl_{>2\ \mu m}$ observed in April. Integrated biomass was however approx. twice more variable than assimilation numbers, thus holding the general covariance between standing stocks and productivity. Increasing PP/chl values as stratification progressed such as we show in Fig. 5B had already been found in temporally more restricted surveys (Morán and Estrada, 2005). This pattern could exacerbate in the coming decades (Capotondi et al., 2012).

Water-column light utilization efficiency values (Ψ) fit within the range given by (Falkowski and Raven, 1997). Similarly to PP/Chl ratios (Fig. 5A), they were also seasonally variable for large cells, although maxima were lagged here towards the end of the year: winter-early spring values (Jan-Apr mean 0.30 g C g chl^{-1} mol $photons^{-1}$ m^2) were considerably lower than late summer-autumn ones (Sep-Dec mean 0.69 g C g chl^{-1} mol $photons^{-1}$ m^2, Fig. 6). Predictability of these productivity indices was higher for large phytoplankton than for the total (Fig. 5A, 6), partially due to the different photosynthetic behaviour of picophytoplankton on the vertical scale (cf. Fig. 2 and Fig. 4 in Morán 2007). Contrary to (Hashimoto and Shiomoto, 2002), higher Ψ values were usually found for picophytoplankton (data not shown) than for large phytoplankton. Seasonality of picophytoplankton Ψ displayed no clear temporal pattern and bore no significant relationship with any of the explored variables, with the most conspicuous difference being that its maximum values (1.1-1.5 g C g chl^{-1} mol photons m^2) were attained from March through May, virtually coincident with the period of large phytoplankton Ψ minima. The well-known seasonal shift in the relative importance of large vs. small phytoplankton biomass (Winder and Cloern 2010) resulted in the opposite in terms of water-column light utilization efficiency during the spring diatom-dominated phytoplankton bloom, likely related with the different response of phytoplankton size-fractions and functional groups to nutrient availability (Kiørboe, 1993; Raven, 1998). Diatoms are the only phytoplankters that need silicate as an essential nutrient. During the spring bloom in April nitrate and silicate concentrations were close or below the half-saturation constant *K*s values and growth values reported for coastal diatom species (Lomas and Glibert, 2000; Egge and Aksnes, 1992), which implies that the diatoms were not growing at their maximum rate (Falkowski et al. 1991). It should be noted that the correlation between average inorganic nutrient concentrations and Ψ, which was significantly positive with phosphate for large cells, dissapeared for picophytoplankton. Although mean concentration of nutrients in the water column are a bulk estimate of nutrient availability at every depth, especially in strongly stratified conditions such as those found between June and October, serious nutrient limitation in the upper mixed layer cannot be overcome by high concentrations below the nutricline. Similarly to PP/Chl ratios, the vertical profiles of phytoplankton abundance (as Chl) could have played a role in the seasonal changes of Ψ, but we should take into consideration that seasonality of PP/Chl ratios and Ψ was completely different for the last third of the year (September to December, cf. Figs. 5 ad 6). Lower individual chlorophyll content in the upper layers in summer is a direct response to higher irradiance but both variables are in the denominator of Ψ, thus partially cancelling each other. Altogether, we suggest that nutrient availability played an

important role in determining the seasonal changes in the water-column light utilization efficiency of large phytoplankton.

Analysis of a decade of data from the station analyzed here plus the other two stations routinely sampled on the continental shelf off Xixón give little support to the existence of bimodal distributions of phytoplankton biomass at this site contrary to other nearby areas (Bode et al., 2011; O'Brien et al., 2012). The lack of a persistent autumn bloom does not mean that PP is only high during the winter-spring transition. Altogether, our results suggest that on the Southern Bay of Biscay continental shelf the diatom spring bloom, although responsible for the highest monthly PP value measured in 2003, does not necessarily translate into sustained high PP values. Rather, PP peaks could be observed sporadically during other low biomass months where light utilization efficiency and production to chlorophyll ratios became maximum. Indeed, bimodal distributions of zooplankton abundance and biomass at the study site (O'Brien et al., 2013) suggest tight grazing responses to both the persistent spring PP peaks and the more sporadic ones found in autumn.

In summary, the annual cycle of planktonic photosynthetic parameters and primary production in the Southern Bay of Biscay continental shelf showed a widely different response and seasonality for small (i.e picophytoplankton, Morán, 2007) and large (nano- plus microplankton, this study) cells. Our analysis shows that monthly variations in primary production at this mesotrophic site are not necessarily well captured by changes in chlorophyll. Total primary production will be better modelled after splitting the phytoplankton assemblage into size classes, with the large fraction apparently more responsive to seasonally predictable factors.

Acknowledgements

We thank A. Calvo-Díaz and Á. Lamas for their help with *P-E* incubations and large phytoplankton analysis. Inorganic nutrients were analyzed by N. González and C. Carballo. This work was financially supported by the Spanish research grant VARIPLACA (CICYT, REN2001-0345/MAR) and the time-series programme RADIALES of the Instituto Español de Oceanografía.

REFERENCES

Basterretxea, G., Arístegui, J., 1999. Phytoplankton biomass and production during late austral spring (1991) and summer (1993) in the Bransfield Strait. Polar Biol. 21, 11-22.

Basterretxea, G., Arístegui, J., 2000. Mesoscale variability in phytoplankton biomass distribution and photosynthetic parameters in the Canary-NW African coastal transition zone. Mar. Ecol. Prog. Ser. 197, 27-40.

Behrenfeld, M.J., Prasil, O., Babin, M., Bruyant, F., 2004. In search of a physiological basis for covariations in light-limited and light-saturated photosynthesis. J. Phycol. 40, 4-25.

Bode, A., Anadón, R., Morán, X.A.G., Nogueira, E., Teira, E., Varela, M., 2011. Decadal variability in chlorophyll and primary production off NW Spain. Climate Research 48, 293-305.

Boyce, D.G., Lewis, M.R., Worm, B., 2010. Global phytoplankton decline over the past century. Nature 466, 591-596.

Butrón, A., Iriarte, A., Madariaga, I., 2009. Size-fractionated phytoplankton biomass, primary production and respiration in the Nervión-Ibaizabal estuary: A comparison with other nearshore coastal and estuarine ecosystems from the Bay of Biscay. Continental Shelf Research 29, 1088-1102.

Capotondi, A., Alexander, M.A., Bond, N.A., Curchitser, E.N., Scott, J.D., 2012. Enhanced upper ocean stratification with climate change in the CMIP3 models. Journal of Geophysical Research-Oceans 117.

Cermeño, P., Marañón, E., Pérez, V., Serret, P., Fernández, E., Castro, C.G., 2006. Phytoplankton size structure and primary production in a highly dynamic. coastal ecosystem (Ria de Vigo, NW-Spain): Seasonal and short-time scale variability. Estuarine Coastal and Shelf Science 67, 251-266.

Claustre, H., Moline, M.A., Prezelin, B.B., 1997. Sources of variability in the column photosynthetic cross section for Antarctic coastal waters. Journal of Geophysical Research-Oceans 102, 25047-25060.

Côté, B., Platt, T., 1983. Day-to-day variations in the spring-summer photosynthetic parameters of coastal marine phytoplankton. Limnol. Oceanogr. 28, 320-344.

Cullen, J.J., Franks, P.J.S., Karl, D.M., Longhurst, A., 2002. Physical influences on marine ecosystem dynamics, in: Robinson, A.R., McCarthy, J.J., Rothschild, B.J. (Eds.), The Sea, Volume 12. John Wiley & Sons, Inc., New York, pp. 299-336.

Cullen, J.J., Lewis, M.R., 1988. The kinetics of photoadaptation in the context of vertical mixing. J. Plankton Res. 10, 1039-1063.

Dower, K.M., Lucas, M.I., 1993. Photosynthesis-irradiance relationships and production associated with a warm-core ring shed from the Agulhas Retroflection south of Africa. Mar. Ecol. Prog. Ser. 95, 141-154.

Estrada, M., 1996. Primary production in the northwestern Mediterranean. Sci. Mar. 60 (Supl. 2), 55-64.

Falkowski, P.G., 1981. Light-shade adaptation and assimilation numbers. J. Plankton Res. 3, 203-216.

Falkowski, P.G., Barber, R.T., Smetacek, V., 1998. Biochemical controls and feedbacks on oceanic primary production. Science 281, 200-206.

Falkowski, P.G., Raven, J.A., 1997. Aquatic photosynthesis. Blackwell Science, Malden, MA.

Fernández, E., Marañón, E., Morán, X.A.G., Serret, P., 2003. Potential causes for the unequal contribution of picophytoplankton to total biomass and productivity in oligotrophic waters. Mar. Ecol. Prog. Ser. 254, 101-109.

Frenette, J.J., Demers, S., Legendre, L., Boule, M., 1996. Size-related photosynthetic characteristics of phytoplankton during periods of seasonal mixing and stratification in an oligotrophic multibasin lake system. J Plankton Res 18, 45-61.

Gameiro, C., Zwolinski, J., Brotas, V., 2011. Light control on phytoplankton production in a shallow and turbid estuarine system. Hydrobiologia 669, 249-263.

Geider, R.J., 1993. Quantitative phytoplankton physiology: implications for primary production and phytoplankton growth. ICES mar. Sci. Symp. 197, 52-62.

Grasshoff, K., Kremling, K., Ehrhardt, M.(Eds.), 1999. Methods of seawater analysis, 3rd ed.Verlag Chemie / Wiley-VCH, Weinheim / NewYork (600pp.).

Hashimoto, S., Shiomoto, A., 2002. Light utilization efficiency of size-fractionated phytoplankton in the subarctic Pacific, spring and summer 1999: high efficiency of large-sized diatom. J Plankton Res 24, 83-87.

Huret, M., Sourisseau, M., Petitgas, P., Struski, C., Leger, F., Lazure, P., 2013. A multi-decadal hindcast of a physical-biogeochemical model and derived oceanographic indices in the Bay of Biscay. Journal of Marine Systems 109, S77-S94.

Ianson, D., Pond, S., Parsons, T., 2001. The spring phytoplankton bloom in the coastal temperate ocean: growth criteria and seeding from shallow embayments. J Oceanogr 57, 723-734.

Joint, I.R., Pomroy, A.J., 1986. Photosynthetic characteristics of nanoplankton and picoplankton from the surface mixed layer. Mar. Biol 92, 465-474.

Jouenne, F., Lefebvre, S., Veron, B., Lagadeuc, Y., 2007. Phytoplankton community structure and primary production in small intertidal estuarine-bay ecosystem (eastern English Channel, France). Mar Biol 151, 805-825.

Kiørboe, T., 1993. Turbulence, phytoplankton cell size and the structure of pelagic food webs. Adv. Mar. Biol. 29, 1-72.

Lewis, M.R., Cullen, J.J., Platt, T., 1984. Relationships between vertical mixing and photoadaptation of phytoplankton: similarity criteria. Mar. Ecol. Prog. Ser. 15, 141-149.

MacIntyre, H.L., Kana, T.M.A., T., Geider, R.J., 2002. Photoacclimation of photosynthesis irradiance response curves and photosynthetic pigments in microalgae and cyanobacteria. J. Phycol. 38, 17-38.

Marty, J.-C., Chiavérini, J., 2002. Seasonal and interannual variations in phytoplankton production at DYFAMED time-series station, northwestern Mediterranean Sea. Deep-Sea Res. II 49, 2017-2030.

Morán, X.A.G., 2007. Annual cycle of picophytoplankton photosynthesis and growth rates in a temperate coastal ecosystem: a major contribution to carbon fluxes. Aquatic Microbial Ecology 49, 267-279.

Morán, X.A.G., Estrada, M., 2001. Short-term variability of photosynthetic parameters and particulate and dissolved primary production in the Alboran Sea (SW Mediterranean). Marine Ecology-Progress Series 212, 53-67.

Morán, X.A.G., Estrada, M., 2005. Winter pelagic photosynthesis in the NW Mediterranean. Deep-Sea Research Part I-Oceanographic Research Papers 52, 1806-1822.

Morán, X.A.G., Taupier-Letage, I., Vázquez-Domínguez, E., Ruiz, S., Arin, L., Raimbault, P., Estrada, M., 2001. Physical-biological coupling in the Algerian Basin (SW Mediterranean): Influence of mesoscale instabilities on the biomass and production of phytoplankton and bacterioplankton. Deep-Sea Research Part I-Oceanographic Research Papers 48, 405-437.

Nixon, S.W., 1995. Coastal Marine Eutrophication - a Definition, Social Causes, and Future Concerns. Ophelia 41, 199-219.

O'Brien, T.D., Li, W.K.W., Moran, X.A.G., (Eds.) 2012. ICES Phytoplankton and Microbial Plankton Status Report 2009/2010, ICES CRR No. 313, 196 pp.

O'Brien, T.D., Wiebe, P.H., Falkenburg, T., (Eds.) 2013. ICES Zooplankton Status Report 2010/2011, ICES CRR No. 318, 108 pp.

Ospina-Alvarez, N., Varela, M., Doval, M.D., Gómez-Gesteira, M., Cervantes-Duarte, R., Prego, R., 2014. Outside the paradigm of upwelling rias in NW Iberian Peninsula: Biogeochemical and phytoplankton patterns of a non-upwelling ria. Estuarine Coastal and Shelf Science 138, 1-13.

Platt, T., Gallegos, C.L., Harrison, W.G., 1980. Photoinhibition of photosynthesis in natural assemblages of marine phytoplankton. J. Mar. Res. 38 (4), 687-701.

Platt, T., Subba Rao, D.W., Irwin, B., 1983. Photosynthesis of picoplankton in the oligotrophic ocean. Nature 301, 702-704.

Raven, J.A., 1998. The twelfth Tansley Lecture. Small is beautiful: the picophytoplankton. Functional Ecology 12, 503-513.

Sakshaug, E., Bricaud, A., Dandonneau, Y., Falkowski, P.G., Kiefer, D.A., Legendre, L., Morel, A., Parslow, J., Takahashi, M., 1997. Parameters of photosynthesis: definitions, theory and interpretation of results. J. Plankton Res. 19, 1637-1670.

Shaw, P.J., Purdie, D.A., 2001. Phytoplankton photosynthesis-irradiance parameters in the near-shore UK coastal waters ot the North Sea: temporal variation and environmental control. Mar. Ecol. Prog. Ser. 216, 83-94.

Steemann-Nielsen, E., 1952. The use of radio-active carbon (^{14}C) for measuring organic production in the sea Journal du Conseil Permanent International pour l'Exploration de la Mer 18, 117-140.

Tilstone, G.H., Figueiras, F.G., Lorenzo, L.M., Arbones, B., 2003. Phytoplankton composition, photosynthesis and primary production during different hydrographic conditions at the Northwest Iberian upwelling system. Mar. Ecol. Prog. Ser. 252, 89-104.

Tillmann, U., Hesse, K.-J., Colijn, F., 2000. Planktonic primary production in the German Wadden Sea. J. Plankton Res. 22, 1253-1276.

Tremblay, J.E., Legendre, L., 1994. A model for the size-fractionated biomass and production of marine phytoplankton. Limnology and Oceanography 39, 2004-2014.

Uitz, J., Huot, Y., Bruyant, F., Babin, M., Claustre, H., 2008. Relating phytoplankton photophysiological properties to community structure on large scales. Limnol Oceanogr 53, 614-630.

Utermöhl, H., 1958. Zur Vervollkommnung der quantitativen Phytoplankton-Methodik. Mitt. Int. Ver. Theor. Angew. Limnol. 9, 1-38.

Varela, M., Prego, R., Pazos, Y., Moroño, A., 2005. Influence of upwelling and river runoff interaction on phytoplankton assemblages in a Middle Galician Ria and comparison with northern and southern rias (NW Iberian Peninsula). Estuarine Coastal and Shelf Science 64, 721-737.

Vollenweider, R.A., Giovanardi, F., Montanari, G., Rinaldi, A., 1998. Characterization of the trophic conditions of marine coastal waters with special reference to the NW Adriatic Sea: Proposal for a trophic scale, turbidity and generalized water quality index. Environmetrics 9, 329-357.

Webb, W.L., Newton, M., Starr, D., 1974. Carbon dioxide exchange of *Alnus rubra*: a mathematical model. Oecologia 17, 281-291.

Winder, M., Cloern, J.E., 2010. The annual cycles of phytoplankton biomass. Philosophical Transactions of the Royal Society B-Biological Sciences 365, 3215-3226.

Table 1. Mean (± SE) annual values of photosynthetic parameters for small (<2 µm) and large (>2 µm) phytoplankton in surface and deep samples of the study site in 2003. Highlighted in bold are significant differences ($p<0.05$, paired *t*-tests) between both size fractions. n=11-12. [a] n=3.

	Surface		Deep	
	Small	Large	Small	Large
α^B [mg C mg chl a^{-1} h^{-1} (µmol photons m^{-2} s^{-1})$^{-1}$]	0.018 (0.002)	0.026 (0.004)	**0.044 (0.008)**	**0.023 (0.003)**
P^B_m (mg C mg chl a^{-1} h^{-1})	5.90 (1.27)	4.94 (0.66)	**4.93 (0.88)**	**2.30 (0.32)**
β^B (same units as α^B)			0.0008[a] (0.0005)	0.0002[a] (0.0001)
E_k (µmol photons m^{-2} s^{-1})	435 (137)	236 (55)	129 (25)	122 (24)

Table 2. Monthly integrated or averaged values (0-75 m) of phosphate and silicate (µmol L^{-1}), total and large (>2 µm) chlorophyll (mg m^{-2}) and primary production rates (mg C m^{-2} d^{-1}) at the sampled station. Also shown are the relative contributions of large phytoplankton to total biomass as chlorophyll (BL/BT) and production rates (PL/PT) and the integrated primary production to chlorophyll ratios for both size fractions (PP/Chl, mg C mg chl^{-1} d^{-1}). [a] Nutrient samples were not available for September.

Date 2003	PO_4	SiO_2	Chl_{tot}	$Chl_{>2\ µm}$	PP_{tot}	$PP_{>2\ µm}$	BL/BT	PL/PT	PP/Chl_{tot}	$PP/Chl_{>2\ µm}$
16 Jan	0.33	1.74	27.9	14.7	214.8	123.9	0.53	0.60	7.7	8.4
17 Feb	0.13	2.77	43.1	23.4	228.9	121.3	0.54	0.47	5.3	5.2
19 Mar	0.10	0.87	25.0	20.5	304.7	122.9	0.82	0.46	12.2	6.0
14 Apr	0.07	1.01	197.7	181.1	891.8	412.82	0.92	0.46	4.5	2.3
13 May	0.04	0.67	22.1	15.1	510.9	229.0	0.68	0.45	23.1	15.2
11 Jun	0.13	0.64	28.8	15.6	131.5	104.9	0.54	0.80	4.6	6.7
14 Jul	0.12	0.59	31.7	17.6	198.1	85.6	0.55	0.43	6.3	4.9
13 Aug	0.14	0.52	23.6	8.6	518.5	201.4	0.37	0.39	22.0	23.3
18 Sep	[a]	[a]	39.8	24.4	656.0	629.0	0.61	0.98	16.5	25.7
15 Oct	0.32	1.82	25.2	9.8	485.4	135.4	0.39	0.28	19.3	13.7
11 Nov	0.03	0.67	37.8	16.2	363.5	148.5	0.43	0.41	9.6	9.2
15 Dec	0.85	2.04	35.8	21.1	150.0	172.4	0.59	1.15	4.2	8.2
Mean	0.21	1.21	44.9	30.7	391.1	207.3	0.58	0.57	11.3	10.7
SE	0.07	0.23	14.0	13.7	67.6	45.8	0.05	0.08	2.1	2.1

Legends to figures

Fig. 1. Monthly variation in the integrated (0-75 m) cell abundance of large phytoplankton groups (A) and their percent contribution (B).

Fig. 2. Monthly variation of the photosynthetic parameters α^B, P^B_m and E_k at the surface and deep waters of the sampled station for the fraction >2 µm (A, C, E) and the total phytoplankton assemblage (B, D, F). In E and F mean values of irradiance measured at the two depths are also given (smaller symbols and dashed lines). The shaded area represents stratifed conditions (i.e. stratification index >0.01 kg m^{-4}). Error bars represent standard errors of the estimates.

Fig. 3. A. Relationship between P^B_m and α^B for the fraction >2 µm (surface and deep sample symbols as in Fig. 2). Fitted OLS linear regression for pooled data: $P^B_m = 0.60 + 124.53\ \alpha^B$, r^2=0.46, p<0.001, n=24. B. Relationship between α^B values of phytoplankton >2 µm and the abundance of diatoms in the samples. Fitted OLS linear regression for pooled data: $\alpha^B = 0.044 - 0.006 + \log \alpha^B$, r^2=0.29, p=0.008, n=23.

Fig. 4. Relationships between the photosynthetic parameters α^B, P^B_m and E_k and the optical depth for pooled data of the fraction >2 µm and the total phytoplankton assemblage. Continuous fitted lines represent significant correlations and include also the relationships for the small fraction described in detail in Morán (2007) (thick grey, total; thick black, >2 µm; thin black, <2 µm) and inlude also the relationship : 0.65** (α^B <2 µm), -0.60** (P^B_m total), -0.66*** (P^B_m >2 µm), -0.56** (E_k total), -0.44* (E_k >2 µm), -0.5* (E_k <2 µm)* p<0.05, ** p<0.01, *** p>0.001, n=24. Dashed lines are non significant correlations showed only for reference.

Fig. 5. A. Monthly variation of the PP/Chl ratios for the fraction >2 µm and total phytoplankton using expected surface irradiances (see the text for details). Fitted line for the fraction >2 µm: $E_{0\ exp}$ $PP/Chl_{>2\ \mu m}$ ratio = $15.81 - 0.50\ day + 5.93 \times 10^{-3}\ day^2 - 2.15 \times 10^{-5}\ day^{3} + 2.38 \times 10^{-8}\ day^{-4}$, r^2=0.71, n=12. B. Relationship between the >2 µm values shown in (A) and the density stratification index (SI) of the water column. Fitted OLS linear regression: $E_{0\ exp}$ $PP/Chl_{>2\ \mu m}$ ratio = 5.80 + 419.1 SI, r^2=0.73, p=0.0002, n=12.

Fig. 6. Monthly variation of water-column light utilization efficiency for total and large phytoplankton. Fitted line for the fraction >2 µm: $0.955 – 0.021\ day + 1.81 \times 10^{-4}\ day^2 - 5.47 \times 10^{-7}\ day^3 + 5.66 \times 10^{-10}\ day^{-4}$ r^2=0.84, n=12.

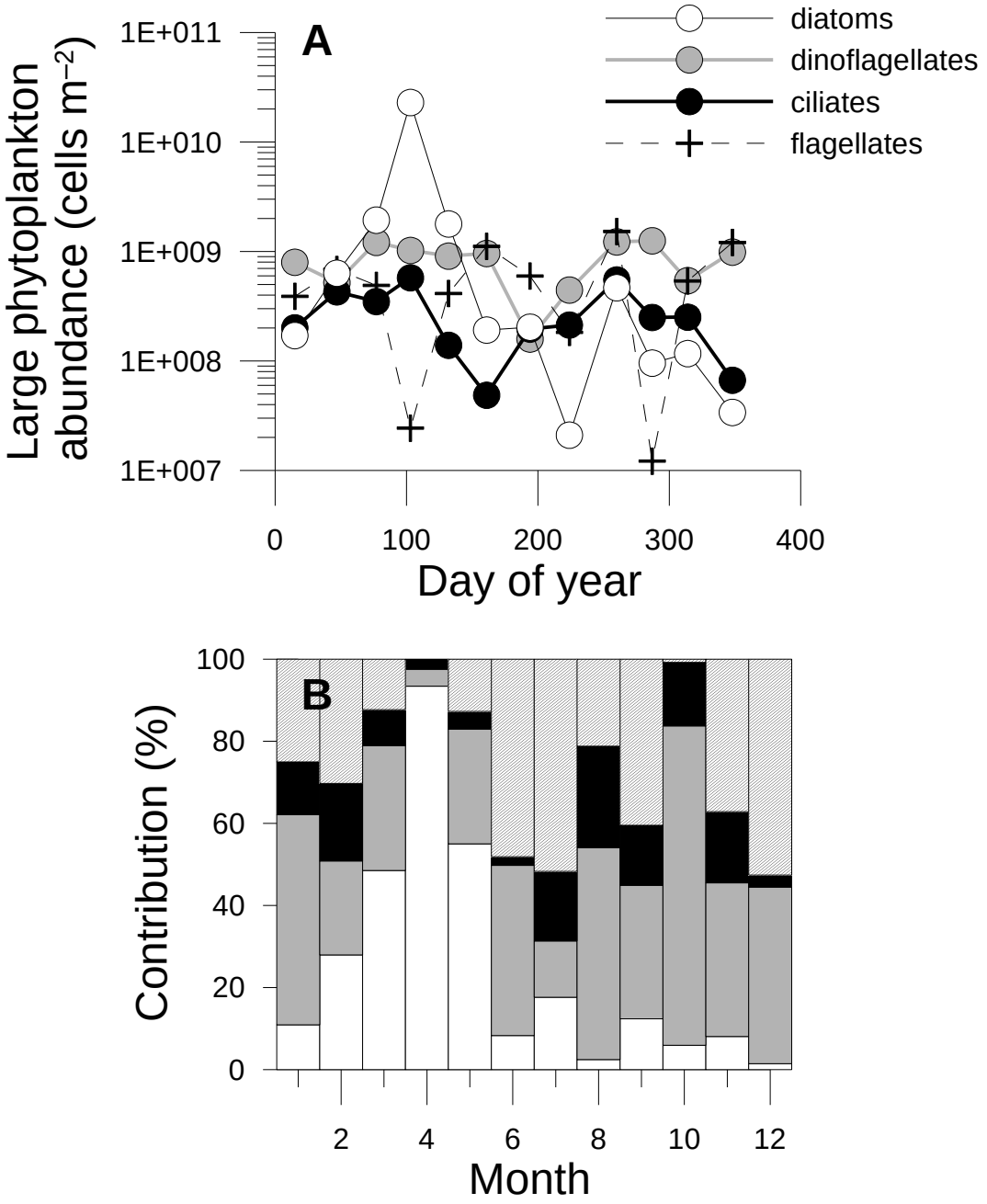
A
diatoms
dinoflagellates
ciliates
flagellates
Large phytoplankton abundance (cells m−2)
1E+011
1E+010
1E+009
1E+008
1E+007
0
100
200
300
400
Day of year
B
Contribution (%)
100
80
60
40
20
0
2
4
6
8
10
12
Month

Fig.1

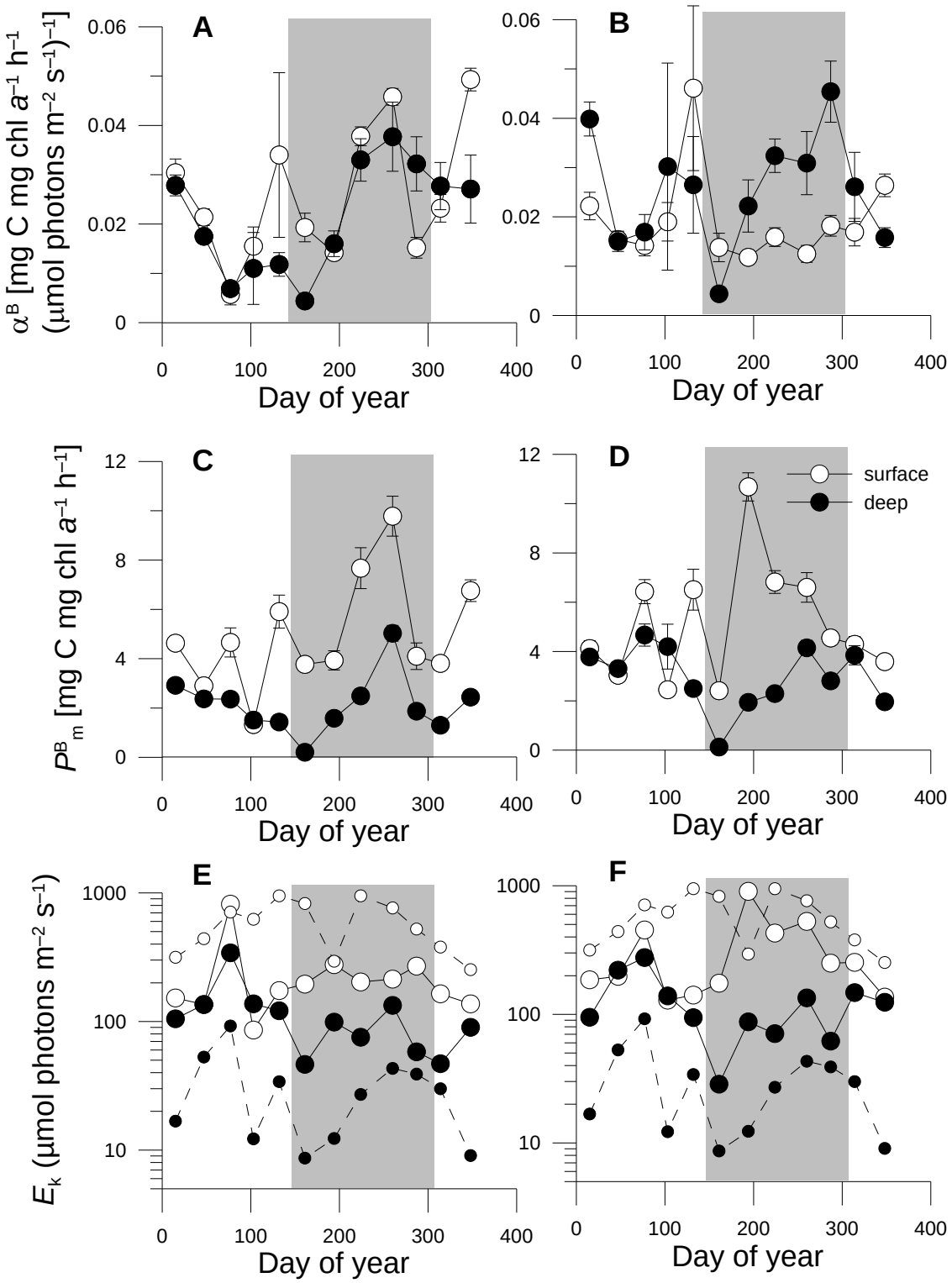
A
B
C
D
E
F
α^B [mg C mg chl a^{-1} h^{-1} (µmol photons m^{-2} s^{-1})$^{-1}$]
P^B_m [mg C mg chl a^{-1} h^{-1}]
E_k (µmol photons m^{-2} s^{-1})
Day of year
surface
deep

Fig. 2

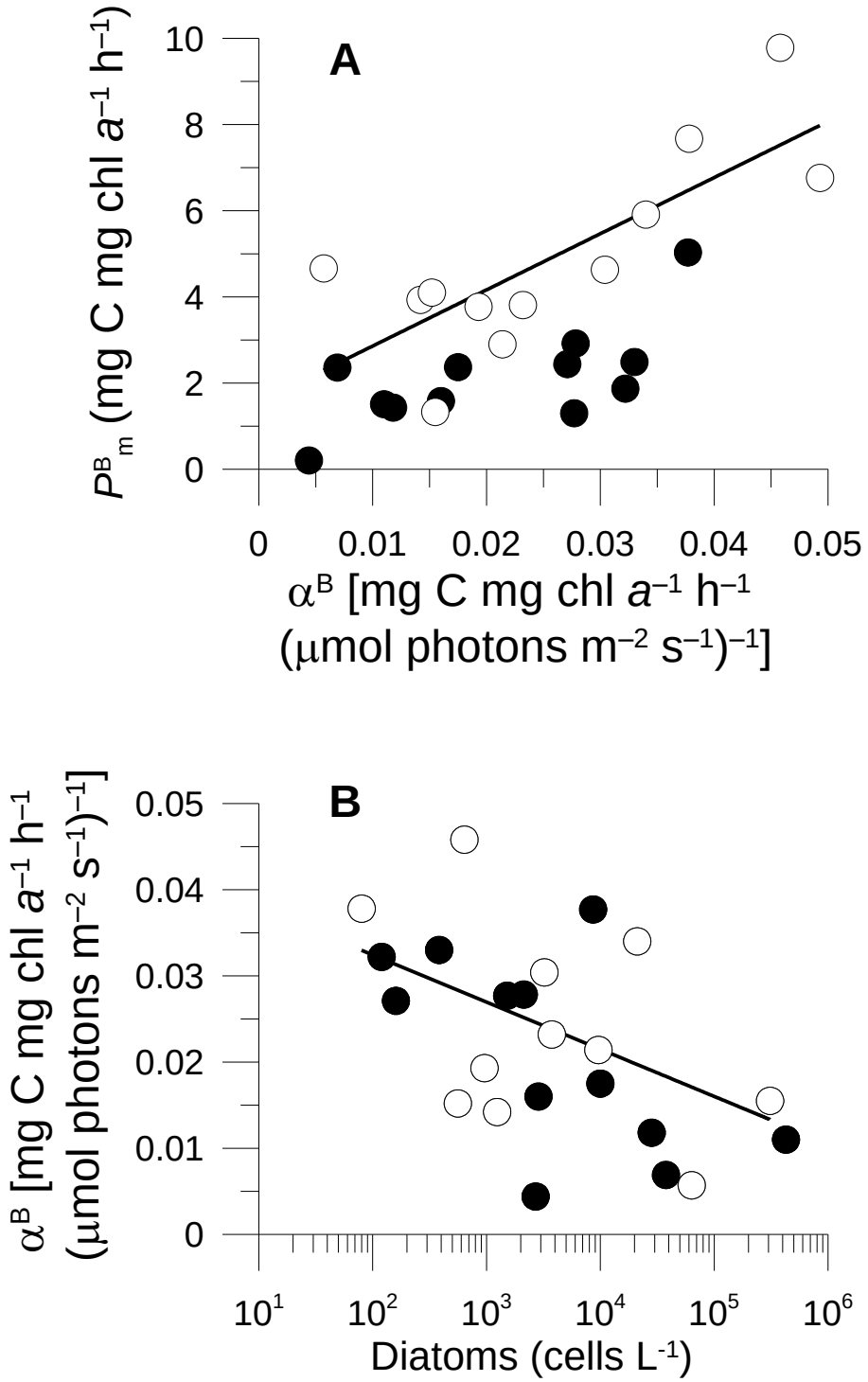
A
B
P^B_m (mg C mg chl a^{-1} h^{-1})
α^B [mg C mg chl a^{-1} h^{-1} (µmol photons m^{-2} s^{-1})$^{-1}$]
Diatoms (cells L^{-1})
0
2
4
6
8
10
0.01
0.02
0.03
0.04
0.05
10^1
10^2
10^3
10^4
10^5
10^6

Fig. 3

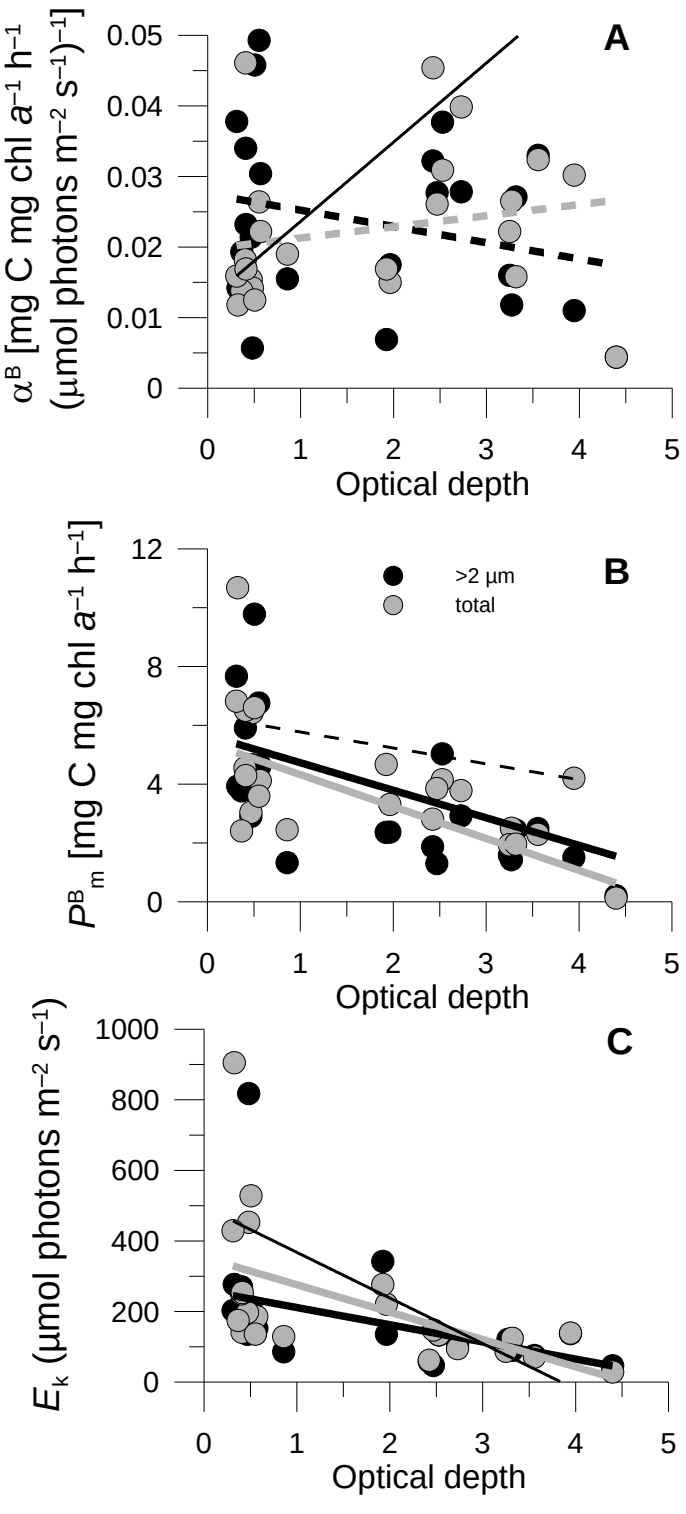
A
α^B [mg C mg chl a^{-1} h^{-1} (µmol photons m^{-2} s^{-1})$^{-1}$]
0.05
0.04
0.03
0.02
0.01
0
0
1
2
3
4
5
Optical depth
B
>2 µm
total
P^B_m [mg C mg chl a^{-1} h^{-1}]
12
8
4
0
0
1
2
3
4
5
Optical depth
C
E_k (µmol photons m^{-2} s^{-1})
1000
800
600
400
200
0
0
1
2
3
4
5
Optical depth

Fig. 4

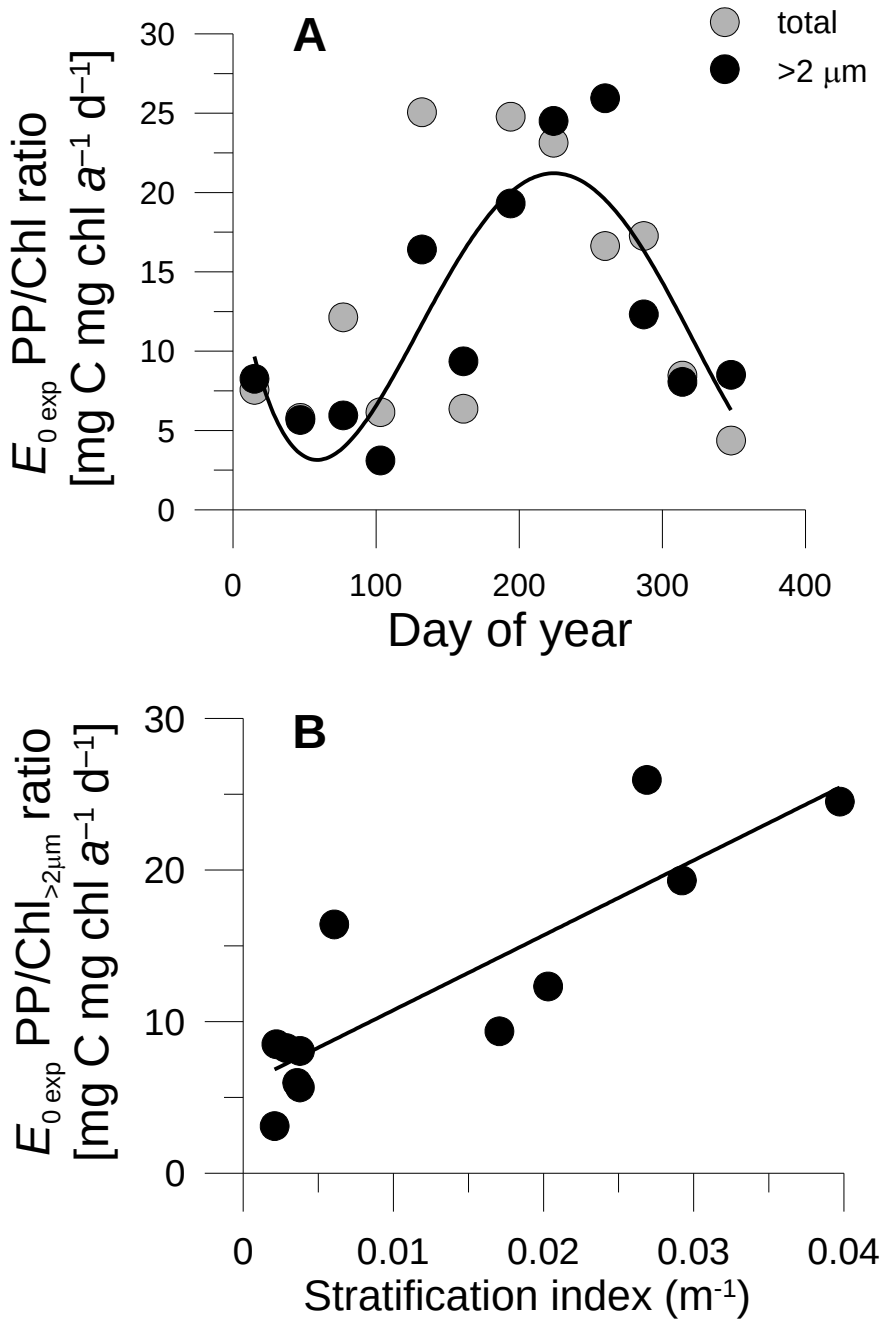
A
total
>2 μm
$E_{0\,exp}$ PP/Chl ratio
[mg C mg chl a^{-1} d^{-1}]
0
5
10
15
20
25
30
0
100
200
300
400
Day of year
B
$E_{0\,exp}$ PP/$Chl_{>2\mu m}$ ratio
[mg C mg chl a^{-1} d^{-1}]
0
10
20
30
0
0.01
0.02
0.03
0.04
Stratification index (m^{-1})

Fig. 5

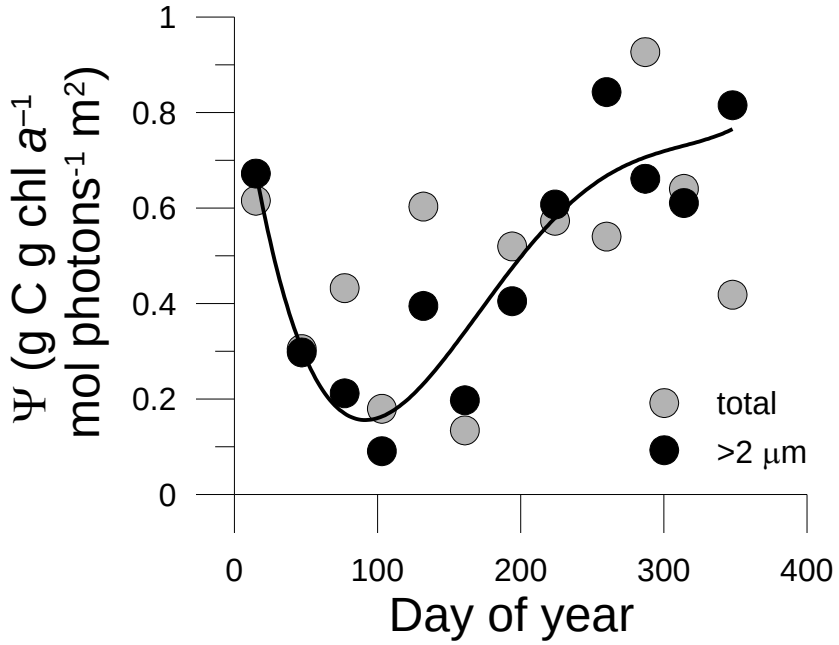
Ψ (g C g chl a⁻¹ mol photons⁻¹ m²)
1
0.8
0.6
0.4
0.2
0
0
100
200
300
400
Day of year
total
>2 μm

Fig. 6